European Journal of Medicinal Chemistry 83 (2014) 674–684

Contents lists available at ScienceDirect

European Journal of Medicinal Chemistry

journal homepage: http://www.elsevier.com/locate/ejmech

Original article

Synthesis and antiproliferative activity of novel methylselenocarbamates

Beatriz Romano [a], María Font [a], Ignacio Encío [b], Juan Antonio Palop [a, *], Carmen Sanmartín [a]

[a] Departamento de Química Orgánica y Farmacéutica, University of Navarra, Irunlarrea 1, E-31008 Pamplona, Spain
[b] Departamento de Ciencias de la Salud, Universidad Pública de Navarra, Avda. Barañain s/n, E-31008 Pamplona, Spain

ARTICLE INFO

Article history:
Received 2 May 2014
Received in revised form
11 June 2014
Accepted 30 June 2014
Available online 1 July 2014

Keywords:
Carbamate
Methylseleno
Cytotoxicity
Apoptosis
Cell cycle arrest

ABSTRACT

A series of new aliphatic, aromatic and heteroaromatic carbamate derivatives containing a methylseleno moiety were synthesized and evaluated *in vitro* for their cytotoxic activity against a panel of human cell lines including CCRF-CEM (lymphoblastic leukaemia), K-562 (lymphocytic leukaemia), HT-29 (colon carcinoma), HTB-54 (lung carcinoma), PC-3 (prostate carcinoma), MCF-7 (breast adenocarcinoma), 184B5 (non-malignant, mammary gland derived) and BEAS-2B (non-malignant, derived from bronchial epithelium). Most of the compounds are highly cytotoxic with GI_{50} values below 10 μM in every tested tumour cell line. Based on its cytotoxic parameters, selectivity index and ADME profile, the biological activity of compound **2**, the propyl derivative, was further analysed in CCRF-CEM and HTB-54 cells. Results showed that this compound is able to induce apoptosis in a time- and dose-dependent manner. Involvement of caspases in cell death induction by **2** was detected. Besides, compound **2** was also able to induce cell cycle arrest at G_0/G_1 in CCRF-CEM cells and at G_2/M in HTB-54 cells.

1. Introduction

Cancer is a serious clinical problem: it affects millions of patients worldwide, reduces life quality and is one of the leading causes of death [1]. At present, there are many antitumour drugs available for clinical use. Despite this fact, treatment of cancer still presents many obstacles and both, lack of selectivity with the consequent side-effects and occurrence of intrinsic or acquired resistance of tumours to chemotherapy point out the necessity to develop new anticancer therapies [2]. In this context, selenium compounds have attracted considerable attention during the last decade since they have been shown to inhibit tumour development and growth in a variety of cancer [3–9]. In particular, converging lines of evidence support the hypothesis that methylselenol is a key intermediate metabolite for effective cancer prevention and treatment by methyl-selenium compounds [10–13].

Over the last years we have been involved in the development, design and synthesis of structurally modified selenium derivatives, some of which exhibited significant cytotoxic and antiproliferative activity through induction of apoptosis, cell cycle arrest and/or modulation of different kinases [14–23]. Among these compounds, we described some methylseleno derivatives whose cytotoxic activity depends on the release of methylselenol [10,14,18,22,24]. Upon this, and considering the chemical structural patterns previously described by us, we designed a general structure for the new compounds presented here. This structure (Fig. 1) keeps a central scaffold of *Se*-methylselenourea, a group whose effectiveness to release methylselenol has been proven. Since carbamates are considered privileged scaffolds in cancer therapy [25–28], keeping a general standard of molecular symmetry [18] and based on a hybrid design approach, here, we try the presence of two carbamate functions attached to this group. Carbamate functions have several roles: first, they act as a link between central and ending scaffolds enabling their chemical accessibility; second, they slightly increase polarity in this area as compared to the structures that we have previously described [14,16,18,21,23]; and third, they theoretically enable the hydrolysis of the compounds towards anionic species that could act as prodrugs. Besides, to explore the influence of the ending pieces of the symmetric molecule on its activity we introduced either an aliphatic or an aromatic structure in these zones.

The use of fatty acids as adjuvants in cancer treatment is well established. *In vitro* studies have displayed the capacity of these

* Corresponding author. Department of Organic and Pharmaceutical Chemistry, University of Navarra, Irunlarrea 1, E-31008 Pamplona, Spain.
E-mail address: jpalop@unav.es (J.A. Palop).

http://dx.doi.org/10.1016/j.ejmech.2014.06.076
0223-5234/

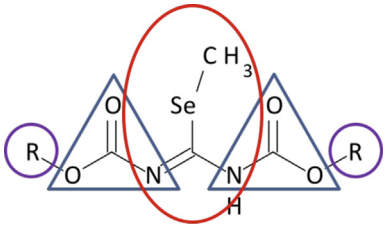

Fig. 1. General structure of new pharmacophoric hybrids.

acids, categorized by the number of carbon atoms in the aliphatic chain, to increase the activity of standard chemotherapeutic agents in a range of cell lines [29–33]. Thus, to juggle with the carbamate group and to imitate the structure of short chain fatty acids, we performed a bioisosteric replacement of a methylene group by an oxygen atom of ether, which causes a slight increase in polarity while keeping a similar bond angle and chain flexibility. Following this approach, here we tested short chain fatty acids (4–7 atoms in length). On the other hand, we selected a series of aromatic rings [14] bearing either one electron-donating group or one electron-withdrawing group to test aromatic endings. These rings were either directly linked to the carbamate, or separated from it by a methylene group. In two cases, the ring was a polycyclic system such as Fmoc [34] or a heteroaromatic unit such as the benzo[*b*]thiophene-1,1-dioxide [35].

Additionally, the cytotoxic activity of every synthesised compound was tested against a panel of six human tumour cell lines as a representative selection of solid, liquid and hormone-dependent tumours, including breast adenocarcinoma (MCF-7), colon carcinoma (HT-29), lymphocytic leukaemia (K-562), lymphoblastic leukaemia (CCRF-CEM), prostate carcinoma (PC-3) and lung carcinoma (HTB-54). As a guide with regard to selectivity, two cell lines derived from non-malignant cells, one from mammary gland (184B5) and the other from bronchial epithelium (BEAS-2B), were also tested. Moreover, to further analyse the mechanism of action of the new compounds, the ability to induce apoptosis and cell cycle arrest of derivative **2**, one of the most active and selective compounds, was also tested.

2. Results and discussion

2.1. Chemistry

The general synthetic route used to obtain the desired bisimidoselenocarbamates was straightforward and it is outlined in Scheme 1. The synthesis was performed from *Se*-methylselenourea hydroiodide, obtained by a method previously developed in our laboratory [18], and the corresponding chloroformates, synthesized according to standard procedures [36,37] or purchased commercially. The reaction was carried out stirring at room temperature for 24–72 h in a 1:2 molar ratio using dried chloroform and in the presence of pyridine. When necessary, dimethylaminopyridine (DMAP) was also included as a basic catalyst. After isolation and purification of the compounds, this procedure gave yields within the range of 5–78%.

Since chloroformates bearing different groups on the aryl ring behave differently, this reaction outcome might be due to the influence of these substituents. For instance, replacement of electron-donating groups on the aromatic ring (**8** and **9**) by electron-withdrawing groups (**10** and **11**) offered a noticeable decrease in yield from 41% to 5%. Moreover, all our attempts to generate the corresponding 4-nitrophenylbiscarbamate were unsuccessful since the reaction of 4-nitrophenylchloroformate with

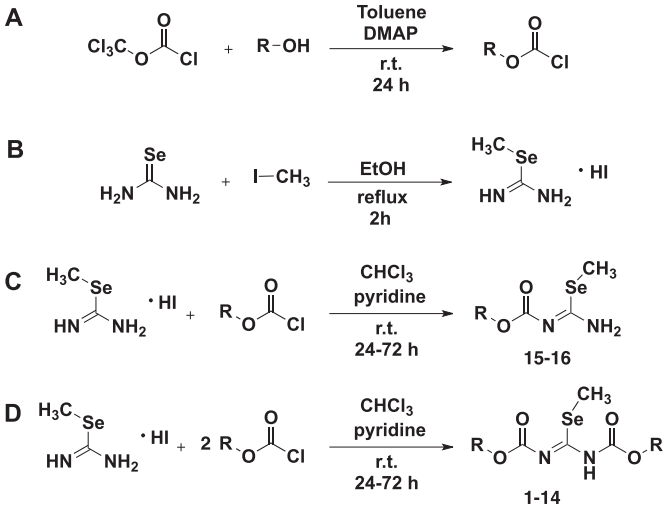

Scheme 1. Synthesis of compounds **1**–**16**. (**A**) Preparation of the corresponding chloroformate. (**B**) Preparation of *Se*-methylselenourea. (**C**) Synthesis of compounds **15**–**16**. (**D**) Synthesis of compounds **1**–**14**.

methylimidoselenocarbamate hydroiodide in different conditions (temperature, solvents, catalyst) always yielded 4-nitrophenol. Hence, to test the influence of the nitro group with regards biological activity, we decided to replace it with a nitrobenzyl group (**13**).

The same traditional synthetic procedure was used for the preparation of the bis derivative of 1,1-dioxobenzo[*b*]thiophenyl. Unfortunately, this procedure failed to afford the expected product and the monomer derivative (**15**) was isolated instead (78% yield). This prompted us to seek alternative routes to prepare the corresponding 1,1-dioxobenzo[*b*]thiophenylbiscarbamate. To our surprise, modification of the reaction conditions (temperature, solvents, molar ratio, catalyst…) resulted in decomposition of both, reagents and monomer yielding complex reaction mixtures.

Despite some of the derivatives (**7**, **10** and **13**) were isolated in a poor yield because their purification was troublesome, all newly synthesized compounds are pure and stable and their structures were confirmed by spectroscopic (IR, ^{1}H NMR and ^{13}C NMR), mass spectrometry (MS) and elemental analysis.

2.2. Biological evaluation

2.2.1. Cytotoxicity

Every synthesised compound was screened for its cytotoxic and antiproliferative activity against CCRF-CEM, K-562, MCF-7, HT-29, PC-3 and HTB-54 cells. Cytotoxicity assays were performed by the MTT [3-(4,5-dimethylthiazol-2-yl)-2,5-diphenyl-tetrazolium bromide] method as previously described [38]. The cytotoxic effect of each substance was tested at five different concentrations between 0.01 and 100 μM. Obtained results are shown in Table 1 and are expressed as GI_{50}, i.e. the concentration that reduces by 50% the growth of treated cells compared to untreated controls, TGI, the concentration that completely inhibits cell growth, and LC_{50}, the concentration that kills 50% of the cells.

As shown in Table 1, CCRF-CEM and HTB-54 cells were generally more sensitive and K-562 more resistant to the cytotoxic effect. In fact, most of the target compounds were active as cytostatic agents against HTB-54, PC-3, CCRF-CEM and MCF-7 cells, with GI_{50} values below 5.5 μM. Moreover, compounds **1**, **2**, **3**, **6**, **7**, **10**, **12** and **15** in HTB-54 cells, **1**, **5**, **7**, and **10** in PC-3 cells, **1**, **2**, **5**, **7**, **9**, **10**, **11**, **12**, **13**, **14**, **15** and **16** in CCRF-CEM cells, **1**, **7**, **10** and **11** in HT-29 cells and **15** in

Table 1
Cytotoxic activities (GI_{50}, TGI and LC_{50} μM) of the compounds in human tumour cell lines.

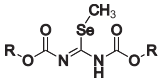

Ref.	R	HTB-54[a]			PC-3[b]			CCRF-CEM[c]			K-562[d]			HT-29[e]			MCF-7[f]		
		GI_{50}	TGI	LC_{50}	GI_{50}	TGI	LC_{50}	GI_{50}	TGI	LC_{50}	GI_{50}	TGI	LC_{50}	GI_{50}	TGI	LC_{50}	GI_{50}	TGI	LC_{50}
1	Ethyl	2.29	6.05	9.81	2.91	5.64	8.37	2.97	5.44	7.91	6.77	39.76	82.10	2.92	6.15	9.37	5.30	9.04	60.17
2	Propyl	2.17	5.67	9.16	5.30	8.91	50.08	2.37	5.07	7.78	2.55	6.18	9.82	9.74	45.44	82.04	4.93	8.02	36.47
3	Butyl	2.74	5.81	8.88	5.30	9.35	53.67	4.38	8.77	48.01	11.65	43.92	76.19	5.13	17.57	65.14	4.78	8.51	45.66
4	Hexyl	22.40	51.96	81.51	5.43	11.24	60.15	7.11	28.41	65.04	21.25	48.62	76.08	6.96	38.53	74.05	5.91	27.02	67.44
5	Isobutyl	2.24	6.73	33.11	3.75	6.25	8.75	3.25	5.97	8.70	5.29	34.46	69.33	3.60	8.24	49.73	7.17	27.77	66.15
6	Allyl	2.41	6.08	9.76	6.68	22.58	63.35	6.95	32.18	66.53	5.06	29.00	65.61	4.43	8.01	43.30	5.17	8.30	43.08
7	Phenyl	2.16	5.66	9.15	3.51	5.98	8.54	2.79	5.26	7.74	4.68	19.16	81.59	2.42	5.41	8.39	4.10	7.97	45.31
8	4-Methoxy-Ph	3.42	7.88	51.18	4.00	7.15	17.87	3.96	7.57	32.54	10.86	48.62	86.39	3.03	7.32	36.97	7.39	26.92	73.12
9	4-Methyl-Ph	2.56	6.55	21.54	6.28	14.14	60.87	2.25	4.99	7.73	5.88	29.93	65.24	4.49	8.13	44.37	5.42	8.44	47.95
10	4-Cl-Ph	2.55	6.09	9.63	3.14	6.06	8.98	3.17	5.57	7.98	7.53	36.99	71.57	2.92	6.24	9.56	5.62	9.27	59.43
11	4-F-Ph	1.41	5.77	12.80	4.12	7.79	34.33	3.24	5.69	8.14	21.80	52.51	83.22	2.27	5.99	9.72	4.93	8.70	58.24
12	Benzyl	2.96	5.90	8.84	20.53	46.53	72.53	1.85	4.70	7.55	4.82	10.72	56.54	11.58	40.41	69.25	5.80	9.80	53.84
13	4-Nitrobenzyl	0.98	36.88	70.71	7.39	33.38	68.72	2.39	5.09	7.79	14.81	43.83	72.85	6.81	34.19	68.71	11.89	42.49	73.09
14	Fmoc	0.91	9.43	54.42	5.95	18.13	60.13	0.70	3.35	7.00	6.08	34.37	69.08	4.17	8.01	39.50	5.23	8.27	37.08
15	Benzodioxo[g]	1.09	5.20	9.30	5.84	11.85	56.72	0.49	2.45	6.47	4.99	28.60	64.70	5.50	14.63	56.25	3.10	5.68	8.26
16	4-Methyl-Ph[g]	2.19	6.50	54.78	5.48	9.59	60.29	2.00	4.93	7.86	4.51	28.57	69.31	6.28	24.87	65.48	4.63	8.22	77.10
	Etoposide[h]	n.d.[i]	n.d.	n.d.	0.63	3.98	79.43	1.58	50.47	89.95	12.59	>100	>100	31.62	>100	>100	19.95	>100	>100
	Cisplatin[h]	9.64	32.73	50.00	5.01	50.12	>100	1.72	>100	>100	5.01	>100	>100	7.95	>100	>100	3.16	>100	>100

[a] Lung carcinoma.
[b] Prostate carcinoma.
[c] Lymphoblastic leukaemia.
[d] Lymphocytic leukaemia.
[e] Colon carcinoma.
[f] Breast adenocarcinoma.
[g] Monosubstituted derivatives.
[h] NCI data (http://dtp.nci.nih.gov/).
[i] No data.

MCF-7 cells exhibited a strong cytotoxic activity with LC_{50} below 10 μM.

Regarding the influence of the side chain, it can be observed that elongation of alkyl chains from ethyl (**1**) to hexyl (**4**) led to a noticeable decrease in cytotoxicity in HTB-54, PC-3, CCR-CEM and HT-29 cells. Moreover, since **5** was cytotoxic for PC-3 and CCRF-CEM cells and cytostatic for HTB-54 cells, while **3** was cytotoxic for HTB-54 cells and cytostatic for PC-3 and CCRF-CEM cells, comparison between butyl (**3**) and isobutyl (**5**) derivatives revealed that activity profiles are also dependent on the presence or absence of a ramification in the alkyl chain. Besides, comparison between propyl (**2**) and allyl (**6**) derivatives revealed that attachment of an unsaturated unit instead of a saturated one resulted in a decrease in cytotoxic activity in PC-3, K-562, CCRF-CEM and MCF-7 cells.

As for compounds bearing aromatic rings, the anticancer activity was unaffected by the nature (electron-donating or electron-withdrawing) of the substituent in the phenyl ring. For instance, replacement of the hydrogen atom (**7**) by a methyl group (**9**) or by a chlorine atom (**10**) yielded GI_{50} values of 4.10, 5.42 and 5.62 μM in MCF-7 cells, 2.79, 2.25 and 3.17 μM in CCRF-CEM cells, 2.42, 4.49 μM and 2.92 μM in HT-29 cells and 2.16, 2.56 and 2.55 μM in HTB-54 cells. Similarly, the presence (**12**) or absence (**7**) of a methylene group as spacer between the carbamic moiety and the phenyl ring had little or no influence on the activity in any of the tumour cell lines.

In order to determine the selectivity index (SI) of the compounds, cytotoxicity of the methylselenocarbamate derivatives was also evaluated against 184B5 and BEAS-2B, two cell lines derived from non-malignant cells (Table 2). The SI was calculated from GI_{50}, TGI and LC_{50} values according to the formula SI = GI_{50} (184B5)/GI_{50} (MCF-7), TGI (184B5)/TGI (MCF-7) and LC_{50} (184B5)/LC_{50} (MCF-7) for breast cells, and SI = GI_{50} (BEAS-2B)/GI_{50} (HTB-54), TGI (BEAS-2B)/TGI (HTB-54) and LC_{50} (BEAS-2B)/LC_{50} (HTB-54) for lung cells. Ratios between 3 and 6 refer to moderate selectivity; ratios greater than 6 indicate high selectivity toward the corresponding cell line, while compounds not meeting either of these criteria rated non-selective [39]. Based upon these parameters, no selectivity was

Table 2
Cytotoxic activities (GI_{50}, TGI and LC_{50} μM) of the compounds in 184B5 and BEAS-2B cells.

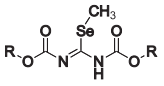

Compound	BEAS-2B[a]			184B5[b]		
	GI_{50}	TGI	LC_{50}	GI_{50}	TGI	LC_{50}
1	3.67	6.22	8.11	3.86	6.01	8.15
2	23.16	48.42	73.68	3.01	5.55	8.09
3	7.22	28.21	65.34	4.15	6.41	8.67
4	25.51	50.56	75.60	5.69	8.99	47.23
5	4.32	6.36	8.39	4.15	6.17	8.19
6	4.05	6.52	9.00	3.22	5.78	8.34
7	4.79	7.00	9.22	4.39	6.47	8.55
8	4.79	7.00	9.22	4.39	6.47	8.55
9	3.52	6.30	9.09	3.82	6.21	8.59
10	3.53	5.75	7.97	4.31	6.31	8.23
11	3.95	5.98	8.01	4.21	6.18	8.16
12	13.50	40.60	67.70	6.12	11.87	55.24
13	3.54	34.35	65.63	5.14	8.51	42.68
14	3.45	5.69	7.94	4.71	7.41	23.69
15	4.96	8.92	44.58	1.32	4.28	7.23
16	6.20	22.55	58.05	3.81	6.24	8.66

[a] Bronchial epithelium cell culture derived from non-malignant cells.
[b] Mammary gland cell culture derived from non-malignant cells.

found with breast cell lines. Compounds **2**, **3**, **12** and **15** however exhibited a good SI in lung cell lines (Table 3).

To compare activity among compounds, GI_{50} MID (average sensitivity of a cell line towards the tested compounds) was calculated and differences against MID for every compound were represented as a mean graph midpoint (MG-MID) (Fig. 2). Most active compounds in a particular cell line of the screen are characterized by a high negative difference to the MID value. Positive values denote smaller activities. Thus, though most of the compounds show up similar activity profiles among cell lines, compounds **2**, **4** and **12** showed a less toxic effect in BEAS-2B cells. Besides, compound **2** (SI 11, 9 and 8 for GI_{50}, TGI and LC_{50} in BEAS-2B) displays the highest negative difference in K-562, the less sensitive cell line to the compounds.

In addition, under our experimental conditions, most of the compounds displayed comparable or higher *in vitro* cytotoxicity values than the traditional anticancer agents cisplatin and etoposide, which were used here as a reference. For example, in HT-29 and MCF-7 cells, the whole series was more active than etoposide. A similar behaviour was observed in HTB-54 cells with the exception of compound **4** (Table 1 and Fig. 2). It is remarkable that in K-562, the least sensitive cell line, compound **2** is five-fold better 8 (in terms of cytotoxicity) than etoposide and two-fold than cisplatin.

Considering its selectivity in lung cells as indicative of a superior therapeutic index and its cytotoxicity on a broad-spectrum of the tested cell lines, compound **2** was selected to further analyse the molecular mechanisms involved in the antiproliferative activity of the new methylselenocarbamates. Curves with the original data from which the GI_{50}, TGI and LC_{50} values for compound **2** were calculated are shown in Fig. 3.

As a filter for drug-like properties, Lipinski descriptors for bioavailability estimation were calculated for compound **2** using the freely accessible program MIPC (Molinspiration Property Calculator) [40]. Obtained results are shown in Table 4. Lipinski parameters describe important molecular properties for drug pharmacokinetics in the human body, especially their oral absorption. According to them, an oral active drug must not violate more than one of the following criteria: <5 hydrogen donors (nOHNH), <10 hydrogen acceptors (nON), MW <500, log Pcalc <5. Moreover, TPSA a predictive indicator of membrane penetration value was also calculated. Results show that compound **2** possess drug like molecule (DLM) features.

Table 3
Selectivity index (SI) of the compounds in lung cell lines.

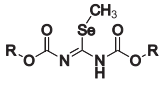

Compound	GI_{50}	TGI	LC_{50}
1	2	1	1
2	11	9	8
3	3	5	7
4	1	1	1
5	2	1	<1
6	2	1	1
7	2	1	1
8	1	1	<1
9	3	3	1
10	1	1	1
11	3	1	1
12	5	7	8
13	4	1	1
14	4	1	<1
15	5	2	5
16	1	1	<1

2.2.2. Determination of apoptosis and effects on cell cycle progression

Apoptosis and cell cycle arrest are two major targets of many anticancer drugs such as doxorubicin and camptothecin. In addition, it is well established that they are mediators of selenium compounds anticancer activity [11,41,42]. To analyse whether the cytotoxic effect caused by compound **2** could be mediated by these events, we evaluated the apoptotic status of the cells and the cell cycle phase distribution in both CCRF-CEM and HTB-54 cell cultures by flow cytometry. With this purpose, Annexin V-FITC and propidium iodide staining for CCRF-CEM cells and the TUNEL technique for HTB-54 cells were used for apoptosis determination and cell cycle evaluation. Cell cultures were treated with 0.5–20 μM of compound **2**, DMSO (vehicle) or 6 μM of Camptothecin, used as a positive control, for 4–48 h. Obtained results are shown in Fig. 4–7.

As can be observed in Figs. 4 and 5, compound **2** was able to induce apoptosis in a time- and dose-dependent manner in both cell lines. For instance, after treatment of CCRF-CEM cell cultures with different amounts of **2** for 24 h, the number of Annexin V positive cells in the cultures rose from 5.2% at 0.5 and 1 μM to 9.6% at 2 μM, 19.8% at 5 μM, 37.8% at 10 μM and 67.3% at 20 μM (Fig. 4B). On the other hand, when the cultures were exposed to 10 μM of **2** the incidence of apoptotic cells at the culture rose from 8.0% after 4 h to 9.8 after 8 h, 37.8 after 24 h and 58.8% after 48 h (Fig. 4C). Similar results were obtained with HTB-54 cells (Fig. 5B and C).

Since caspases play a vital and active role at the initiation and execution of the apoptotic process [43], to assess whether caspases were involved or not in the process of cell death induced by **2**, the apoptotic status of the cells in CCRF-CEM cell cultures treated for 1 h with 50 μM z-VAD-fmk followed by 24 h of exposure to 10 μM of **2** was determined. As shown in Fig. 4D pretreatment with z-VAD-fmk decreased the percentage of apoptotic cells from 36.5% to 14% thus confirming the involvement of caspases in cell death induction by **2**.

Cell cycle distribution of CCRF-CEM cell cultures treated with **2** is shown in Fig. 6. As shown, an increase of the hypodiploid $subG_1$ population could be detected after 24 h of exposure to 5 μM **2** or higher, a result that confirms its ability to induce apoptosis (Fig. 6B). At the same time, a significant increase in G_0/G_1 cell population, as well as a reduction of the S and G_2/M cell populations were detected, thus suggesting cell cycle arrest at G_0/G_1. Time course analysis of cell cycle distribution in CCRF-CEM cell cultures upon treatment with 10 μM of compound **2** confirmed a cell cycle arrest at G_0/G_1 at 24 and 48 h (Fig. 6C).

A parallel study carried out in HTB-54 cells also displayed that **2** is able to induce disturbances in cell cycle in a time and dose dependent manner (Fig. 7). Thus, while low concentrations of **2** (1–2 μM) failed to block cell cycle progression after 24 h, 5 and 10 μM treatment with **2** increased the percentage of S and G_2/M cells whilst decreasing the G_0/G_1 cell population, indicating blockage of the cycle at G_2/M. Additionally, both exposure to 20 μM of **2** and longer incubation times led to a strong increase in the $subG_1$ cell population associated with a reduction in the size of the other phases. These data suggest that cells were not able to recover cell damage.

3. Conclusions

Our recent studies on the research and development of new antitumoural agents led us to identify the methylseleno entity as determinant for the biological activity. In this paper, we show that a number of new methylselenocarbamates hybrids (**1**–**16**) display

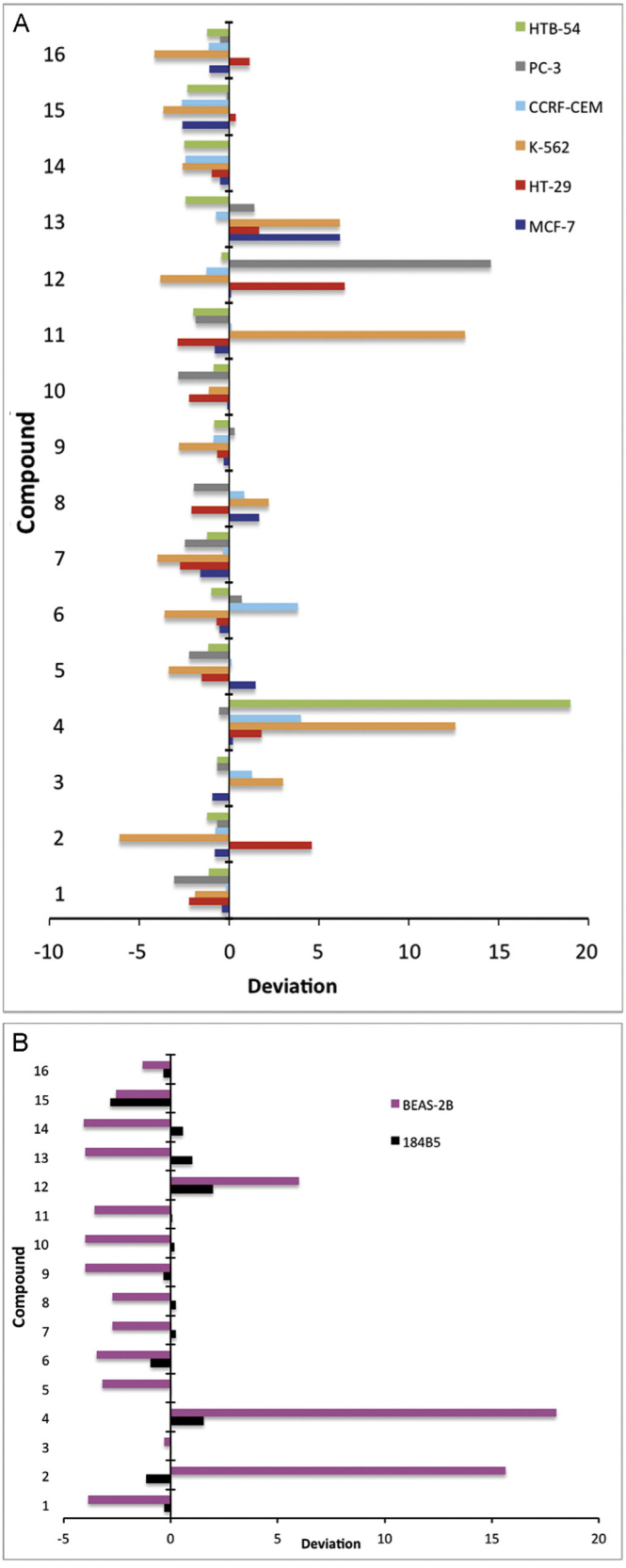

Fig. 2. MG-MID for compounds **1**–**16** in tumour (**A**) and non-malignant cell lines (**B**). Compounds are depicted at the vertical axis. Horizontal bars represent the deviation respect GI_{50} MG-MID value. Compounds with a horizontal bar pointing to the right (positive values) have a GI_{50} that is bigger than the mean, whereas horizontal bars pointing to the left (negative values) indicate GI_{50} values smaller than the mean.

high cytotoxicity against a broad spectrum of human cancer cell lines with GI_{50} values below 10 μM for many of them. Compound **2**, with a good selectivity index in lung cells was selected for additional pharmacological studies. Results showed that **2** induced a caspase-mediated process of cell death that is time and dose dependent. Besides, compound **2** was also able to induce cell cycle arrest at G_0/G_1 in CCRF-CEM cells and at G_2/M in HTB-54 cells. The potent anticancer activity, synthetic accessibility and potential selectivity of these compounds strongly encourage us to continue the development and testing of novel methylselenocarbamate hybrids aimed at investigating their structure–activity relationship and pharmacological mechanism(s) of action.

4. Experimental protocols

4.1. Chemistry

Melting points were determined with a Mettler FP82 + FP80 apparatus (Greifense, Switzerland) and have not been corrected. The ^{1}H and ^{13}C NMR spectra were recorded on a Bruker 400 Ultrashield™ spectrometer (Rheinstetten, Germany) using TMS as the internal standard. The IR spectra were obtained on a Thermo Nicolet FT-IR Nexus spectrophotometer with KBr or NaCl pellets. Elemental microanalyses were carried out on vacuum-dried samples using a LECO CHN-900 Elemental Analyzer. Silica gel 60 (0.040–0.063 mm) 1.09385.2500 (Merck KGaA, 64271 Darmstadt, Germany) was used for Column Chromatography and Alugram® SIL G/UV_{254} (Layer: 0.2 mm) (Macherey–Nagel GmbH & Co. KG. Postfach 101352, D-52313 Düren, Germany) was used for Thin Layer Chromatography. Chemicals were purchased from E. Merck (Darmstadt, Germany), Scharlau (F.E.R.O.S.A., Barcelona, Spain), Panreac Química S.A. (Montcada i Reixac, Barcelona, Spain), Sigma–Aldrich Química, S.A. (Alcobendas, Madrid, Spain), Acros Organics (Janssen Pharmaceuticalaan 3a, 2440 Geel, Belgium) and Lancaster (Bischheim-Strasbourg, France).

4.1.1. General procedure for compounds *1*–*6*

A solution of the corresponding chloroformate (8.08 mmol) in dry chloroform (25 mL) was slowly added dropwise to a stirred

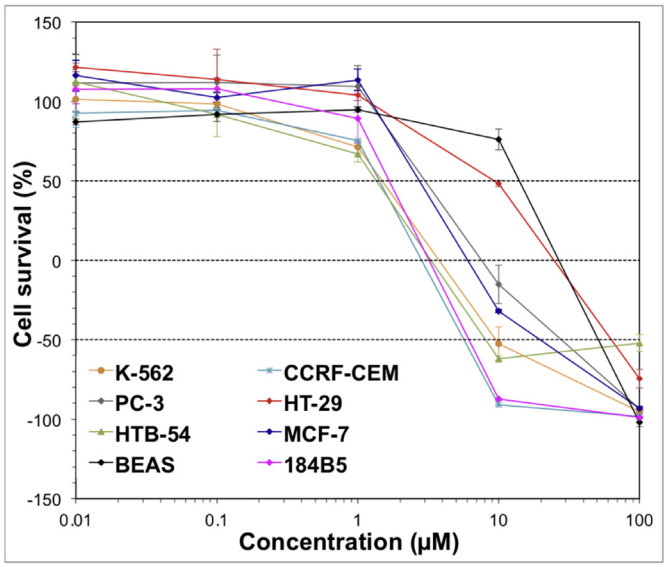

Fig. 3. Cytotoxicity of compound **2** in human cell lines. Cytotoxicity was determined by a colorimetric microassay based on the use of MTT as described in the Experimental protocols Section. Data are expressed as the percentage of growth ± SEM of at least 3 independent experiments performed in quadruplicate.

Table 4
Theoretical structural properties of compound **2**.

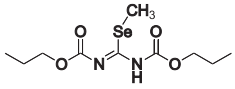

Comp.	log *P*	MW	TPSA	n-OH acceptors	n-OHNH donors	Volume
2	2.56	309	77.00	6	1	244.61

solution of *Se*-methylselenourea (3.94 mmol) in dry chloroform (25 mL) and pyridine (2.5 mL). The mixture was stirred for 24–72 h at room temperature. Water was added to the reaction and the mixture was extracted with dichloromethane (3 × 20 mL). The organic layer was washed with water (3 × 20 mL), dried with Na_2SO_4 and the solvents were removed under vacuum by rotatory evaporation and the residue was treated with ethyl ether (100 mL).

*4.1.2. Methyl N,N′-bis(ethoxycarbonyl)imidoselenocarbamate (**1**)*

From ethyl chloroformate. Yellow solid; mp: 67–70 °C. Yield: 49%. IR (KBr) cm^{-1}: 3228 (N–H), 2983–2931 (C–H_{alif}), 1802 (C=O), 1653 (C=N). ^1H NMR (400 MHz, $CDCl_3$) δ: 1.35 (t, 6H, $2CH_3$, $J_{CH_2-CH_3}$ = 7.1 Hz); 2.3 (s, 3H, $SeCH_3$); 4.26 (c, 4H, $2CH_2$, $J_{CH_2-CH_3}$ = 7.1 Hz), 11.95 (s, 1H, NH) ^{13}C NMR (100 MHz, $CDCl_3$) δ: 8.4 (1C, $SeCH_3$); 14.9 (2C, $2CH_3$); 62.6 (2C, $2CH_2$); 148.9 (1C, CONH); 153.0 (1C, CON); 162.6 (1C, CSe). MS (*m*/*z* % abundance): 282 (M^+•, 14), 191 (19), 177 (100), 159 (52), 149 (19), 132 (71), 115 (44), 105 (43), 88 (40), 69 (38), 57 (33). Elemental Analysis for $C_8H_{14}N_2O_4Se$, Calcd/Found (%): C: 34.16/34.74; H: 4.98/5.09; N: 9.96/10.11.

*4.1.3. Methyl N,N′-bis(propoxycarbonyl)imidoselenocarbamate (**2**)*

From propyl chloroformate. Yellow oil. Yield: 29%. IR (NaCl) cm^{-1}: 3167 (N–H), 2969 (C–H_{alif}), 1747 (C=O), 1651 (C=N). ^1H NMR (400 MHz, $CDCl_3$) δ: 0.96 (t, 6H, 2 CH_3, $J_{CH_3-CH_2}$ = 7.0 Hz); 1.72 (dd, 4H, $2\beta CH_2$ $J_{CH_3-CH_2}$ = 7.0 Hz, $J_{CH_2-CH_2}$ = 14.0 Hz); 2.28 (s, 3H, $SeCH_3$); 4.14 (t, 4H, $2\alpha CH_2$, $J_{CH_2-CH_2}$ = 6.0 Hz); 11.90 (s, 1H, NH). ^{13}C NMR (100 MHz, $CDCl_3$) δ: 10.6 (1C, $SeCH_3$); 13.2 (2C, $2CH_3$); 24.5 (2C, $2\beta CH_2$); 70.5 (2C, $2\alpha CH_2$); 155.3 (1C, CONH); 162.3 (1C, CON); 164.6 (1C, CSe). MS (*m*/*z* % abundance): 311 (M^+•, 30), 251 (16), 215 (7), 129 (75), 46 (87), 69 (19), 43 (100), 27 (16). Elemental Analysis for $C_{10}H_{18}N_2O_4Se$, Calcd/Found (%): C: 38.84/38.96; H: 5.87/5.51; N: 9.06/9.31.

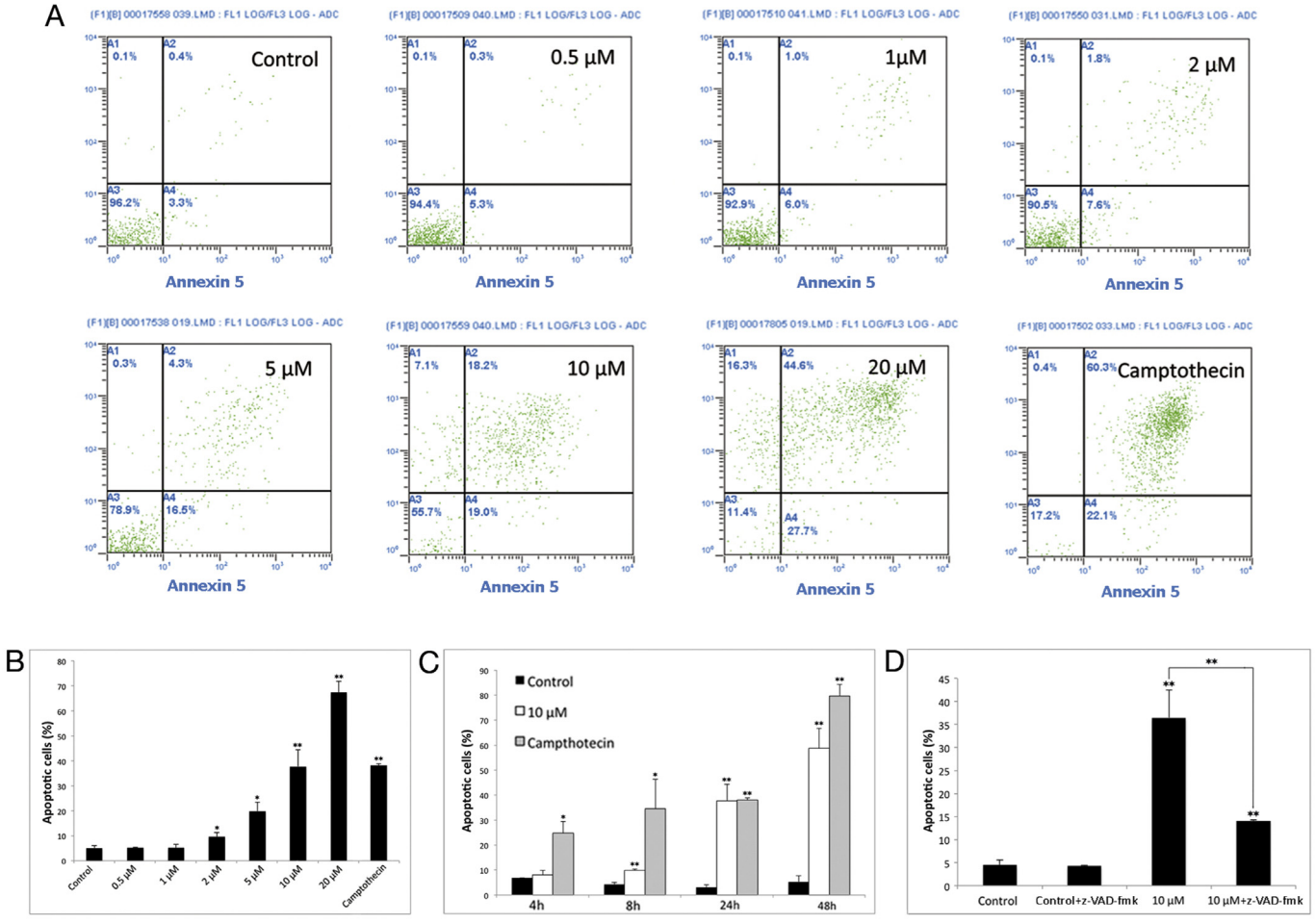

Fig. 4. Analysis of cell death induction in CCRF-CEM cells by compound **2**. Apoptosis was determined by Annexin V-FITC staining as described in Experimental protocols. (**A**) Flow cytometry analysis of a representative experiment after 24 h incubation of the cells in the presence or absence (control) of **2**. (**B**) Percentage of apoptotic cells in the cultures after incubation of the cells either with **2** (0.5–20 μM) or vehicle (control) for 24 h. (**C**) Time course analysis of cell death induction by compound **2** (10 μM). (**D**) Prevention of cell death induction by the pan-caspase inhibitor z-VAD-fmk. Cells were pre-incubated for 1 h either with or without 50 μM z-VAD-fmk and then with 10 μM of **2** for 24 h. Camptothecin was used as a positive control. Results are presented as the mean ± SEM of three independent experiments performed in duplicate. $^*p < 0.05$ and $^{**}p < 0.01$ respect to control cells.

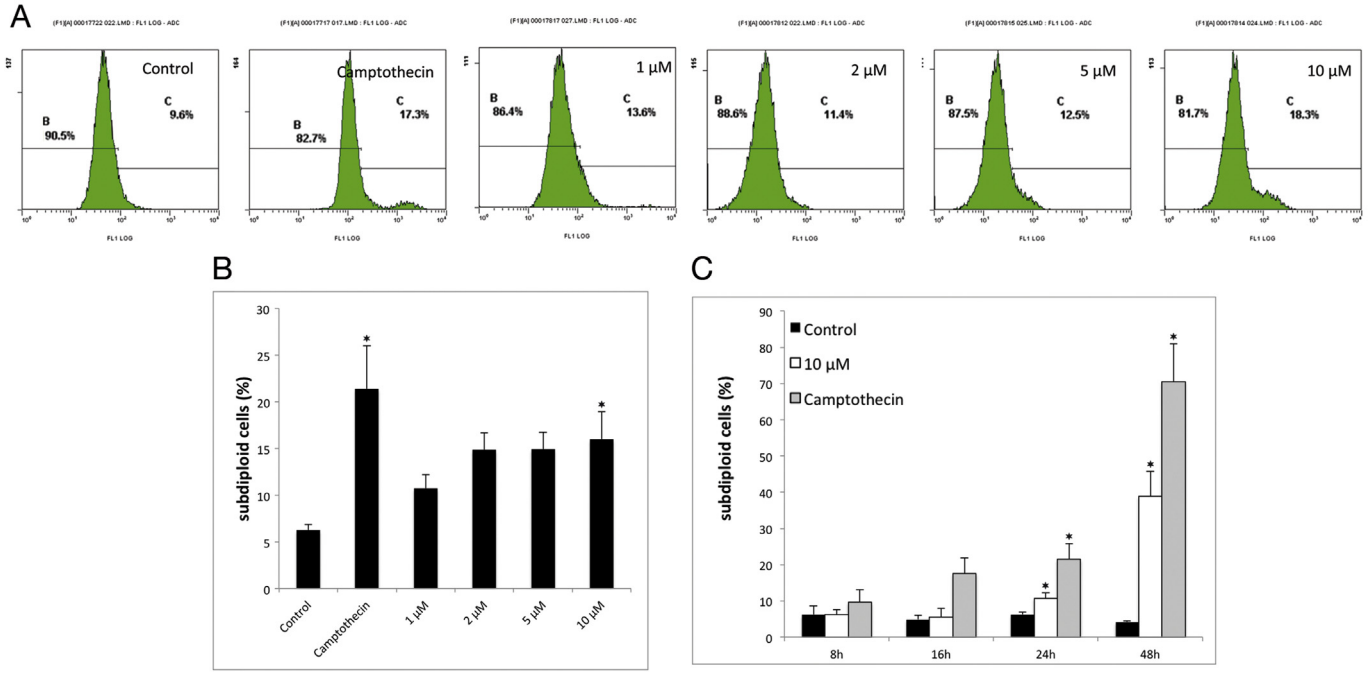

Fig. 5. Analysis of cell death induction in HTB-54 cells by compound **2**. Apoptosis was determined by TUNEL as described in Experimental protocols. (**A**) Flow cytometry analysis of a representative experiment after 24 h incubation of the cells in the presence or absence (control) of **2**. (**B**) Percentage of subdiploid cells in the cultures after incubation of the cells either with **2** (1–10 μM) or vehicle (control) for 24 h. (**C**) Time course analysis of cell death induction by compound **2** (10 μM). Camptothecin was used as a positive control. Results are presented as the mean ± SEM of three independent experiments performed in duplicate. $^{*}p < 0.05$ respect to control cells.

*4.1.4. Methyl N,N′-bis(butoxycarbonyl)imidoselenocarbamate (**3**)*

From butyl chloroformate. Yellow oil. Yield: 74%. IR (NaCl) cm^{-1}: 3167 (N–H), 2961 (C–H_{alif}), 1748 (C=O), 1652 (C=N). ^1H NMR (400 MHz, $CDCl_3$) δ: 0.96 (t, 6H, 2 CH_3, $J_{CH_3-CH_2} = 7.0$ Hz); 1.42 (dq, 4H, 2γCH_2, $J_{CH_3-CH_2} = 7.0$ Hz, $J_{\gamma CH_2-\beta CH_2} = 14$ Hz); 1.70 (dt, 4H, 2βCH_2, $J_{\beta CH_2-\alpha CH_2} = 6.0$ Hz, $J_{\beta CH_2-\gamma CH_2} = 14.0$ Hz); 2.30 (s, 3H, $SeCH_3$); 4.20 (t, 4H, 2αCH_2, $J_{\alpha CH_2-\beta CH_2} = 6.0$ Hz); 11.79 (s, 1H, NH). ^{13}C NMR (100 MHz, $CDCl_3$) δ: 8.4 (1C, $SeCH_3$); 14.4 (2C, $2CH_3$); 19.3 (2C, 2γCH_2); 31.0 (2C, 2βCH_2); 66.2 (2C, 2αCH_2); 153.1 (1C, CONH); 160.1 (1C, CON); 162.6 (1C, CSe). MS (*m/z* % abundance): 338 (M^+•, 3), 306 (14), 279 (17), 253 (15), 206 (31), 191 (12), 179 (27), 153 (20), 126 (15), 111 (15), 69 (36), 57 (100). Elemental Analysis for $C_{12}H_{22}N_2O_4Se$, Calcd/Found (%): C: 42.73/42.66; H: 6.53/6.63; N: 8.31/8.05.

*4.1.5. Methyl N,N′-bis(hexyloxycarbonyl)imidoselenocarbamate (**4**)*

From hexyl chloroformate. Yellow oil. Yield: 74%. IR (NaCl) cm^{-1}: 3163 (N–H), 2956–2930 (C–H_{alif}), 1748 (C=O), 1653 (C=N). ^1H NMR (400 MHz, $CDCl_3$) δ: 0.90 (t, 6H, 2 CH_3, $J_{CH_3-CH_2} = 7.0$ Hz); 1.36 (m, 8H, 2δ + 2εCH_2); 1.38 (m, 4H, 2γCH_2); 1.71 (t, 6H, 2βCH_2, $J_{\beta CH_2-\gamma CH_2} = J_{\beta CH_2-\alpha CH_2} = 7.0$ Hz); 2.30 (s, 3H, $SeCH_3$); 4.18 (t, 4H, 2αCH_2, $J_{\alpha CH_2-\beta CH_2} = 7.0$ Hz); 11.79 (s, 1H, NH). ^{13}C NMR (100 MHz, $CDCl_3$) δ: 6.9 (1C, $SeCH_3$); 13.2 (2C, $2CH_3$); 21.5 (2C, 2εCH_2); 27.5 (2C, 2δCH_2); 39.0 (2C, 2γCH_2); 65.5 (2C, 2βCH_2); 66.7 (2C, 2αCH_2); 151.7 (1C, CONH); 154.2 (1C, CON); 162.0 (1C, CSe). MS (*m/z* % abundance): 394 (M^+•, 6), 171 (37), 85 (100), 69 (19), 57 (45). Elemental Analysis for $C_{16}H_{30}N_2O_4Se$, Calcd/Found (%): C: 48.45/48.50: H: 7.68/7.84; N: 7.12/6.80.

*4.1.6. Methyl N,N′-bis(isobutoxycarbonyl)imidoselenocarbamate (**5**)*

From isobutyl chloroformate. Yellow oil. Yield: 62%. IR (NaCl) cm^{-1}: 3167 (N–H), 2963 (C–H_{alif}), 1749 (C=O), 1652 (C=N). ^1H NMR (400 MHz, $CDCl_3$) δ: 0.95 (d, 12H, 4CH_3, $J_{CH_3-CH} = 6.7$ Hz); 2.0 (m, 2H, 2CH); 2.28 (s, 3H, $SeCH_3$); 4.32 (d, 4H, 2CH_2, $J_{CH_2-CH} = 6.7$ Hz), 11.51 (s, 1H, NH). ^{13}C NMR (100 MHz, $CDCl_3$) δ: 8.4 (1C, $SeCH_3$); 19.6 (4C, 4CH_3); 28.0 (2C, 2CH); 72.6 (2C, 2CH_2); 153.1 (1C, CONH); 160.1 (1C, CON); 162.5 (1C, CSe). MS (*m/z* % abundance): 337 (M^+•, 2), 279 (25), 253 (27), 205 (14), 179 (36), 153 (27), 69 (15), 57 (100). Elemental Analysis for $C_{12}H_{22}N_2O_4Se$, Calcd/Found (%): C: 42.73/42.77; H: 6.53/6.53; N: 8.31/8.36.

*4.1.7. Methyl N,N′-bis(allyloxycarbonyl)imidoselenocarbamate (**6**)*

From allyl chloroformate. Yellow oil. Yield: 21%. IR (NaCl) cm^{-1}: 3168 (N–H), 2937 (C-H_{alif}), 1749 (C=O), 1652 (C=N). ^1H NMR (400 MHz, $CDCl_3$) δ: 2.31 (s, 3H, $SeCH_3$); 4.69 (d, 4H, 2 CH_2, $J_{CH_2=CH} = 6.0$ Hz); 5.31 (d, 2H, 2 CH = , $J_{CHgem-CHcis} = 10.0$ Hz); 5.37 (d, 4H, 2αCH_2, $J_{CH_2-CH} = 6.0$ Hz); 11.94 (s, 1H, NH). ^{13}C NMR (100 MHz, $CDCl_3$) δ: 10.7 (1C, $SeCH_3$); 69.5 (2C, 2CH_2); 121.3 (2C, 2CH_2=); 135.2 (2C, 2CH=); 154.9 (1C, CONH); 161.7 (1C, CON); 164.1 (1C, CSe). MS (*m/z* % abundance): 307 (M^+•, 15), 291 (8), 249 (10), 211 (6), 167 (14), 138 (8), 123 (15), 90 (21), 81 (24), 69 (19), 41 (100). Elemental Analysis for $C_{10}H_{14}N_2O_4Se$, Calcd/Found (%): C: 39.35/39.80; H: 4.62/4.36; N: 9.18/9.31.

*4.1.8. General procedure for compounds **7**–**14** and **16***

A solution of the corresponding chloroformate (8.08 mmol) in dry chloroform (25 mL) was slowly added dropwise to a stirred solution of *Se*-methylselenourea (3.94 mmol) in dry chloroform (25 mL) and pyridine (2.5 mL). For compounds **9**, **12** and **16** dimethylaminopyridine (8.08 mmol) was added. The mixture was stirred for 24–72 h at room temperature. Solvents were removed under vacuum by rotatory evaporation and the residue was treated and purified.

Phenyl chloroformate and 4-methoxyphenyl chloroformate were prepared from phenol or 4-methoxyphenol respectively, and trichloromethylchloroformate in toluene as solvent and with DMAP as catalyst according to the literature [37].

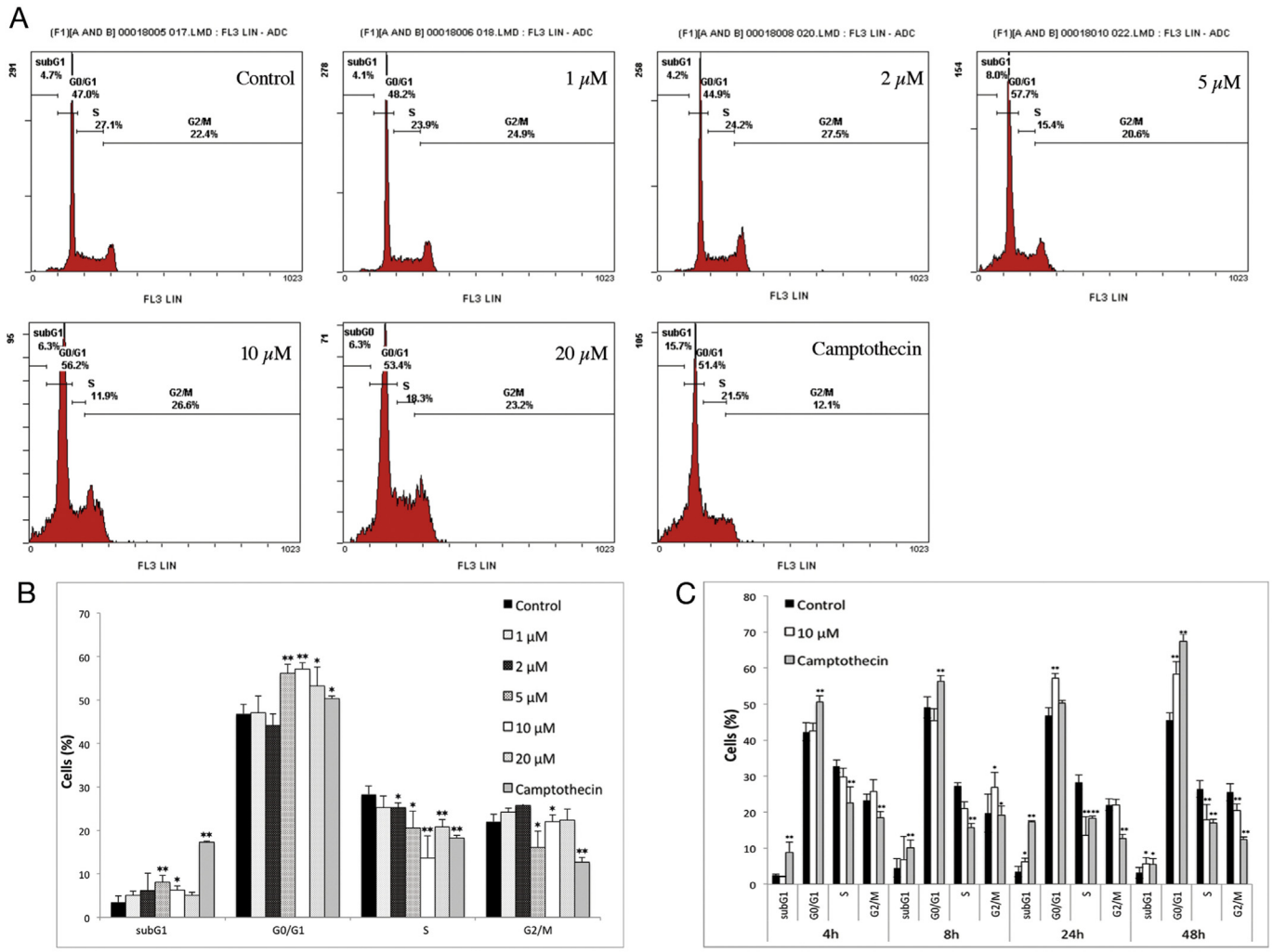

Fig. 6. Effect of compound **2** on cell cycle phase distribution in CCRF-CEM cells. Cells treated with compound **2** were processed for propidium iodide staining and cellular DNA content determined by flow cytometry. (**A**) Flow cytometry analysis of a representative experiment performed with cells treated with 1–20 μM compound **2** or vehicle (control) for 24 h. (**B**) Percentage of cells in each phase of the cell cycle after incubation of the cells in the presence or absence (control) of **2** (1–20 μM) for 24 h. (**C**) Time course analysis of cell cycle phase distribution of CCRF-CEM cell cultures treated with 10 μM of **2**. Camptothecin was used as a positive control. Results are presented as the mean ± SEM of three independent experiments performed in duplicate. $^{*}p < 0.05$ and $^{**}p < 0.01$ respect to control cells.

*4.1.9. Methyl N,N′-bis(phenoxycarbonyl)imidoselenocarbamate (**7**)*

From phenyl chloroformate. The residue was treated with toluene (3 × 20 mL), washed with water (100 mL) and recrystallized from ethanol. A white powder was obtained; mp: 110–112 °C. Yield: 8%. IR (KBr) cm^{-1}: 3430 (N–H), 1751 (C=O), 1670 (C=N). ^1H NMR (400 MHz, $CDCl_3$) δ: 2.33 (s, 3H, $SeCH_3$); 7.20 (d, 4H, $2H_2 + 2H_6$, $J_{2-3} = J_{6-5} = 7.0$ Hz); 7.28 (t, 2H, H_4, $H_{4'}$, $J_{4-3} = J_{4-5} = 7.0$ Hz); 7.44 (m, 4H, $H_3 + H_5$, $H_{3'} + H_{5'}$); 11.97 (s, 1H, NH). ^{13}C NMR (100 MHz, $CDCl_3$) δ: 11.0 (1C, $SeCH_3$); 116.6 (4C, $2C_2 + 2C_6$); 127.0 (6C, $2C_3 + 2C_4 + 2C_5$); 140.4 (2C, $2C_1$); 153.1 (1C, CONH); 160.1 (1C, CON); 164.7 (1C, CSe). MS (*m/z* % abundance): 377 (M^+), 285 (49), 223 (17), 191 (96), 123 (17), 94 (100), 77 (47), 65 (38). Elemental Analysis for $C_{16}H_{14}N_2O_4Se$, Calcd/Found (%): C: 50.93/51.22; H: 3.71/3.72; N: 7.43/7.46.

*4.1.10. Methyl N,N′-bis(4-methoxyphenoxycarbonyl) imidoselenocarbamate (**8**)*

From 4-methoxyphenyl chloroformate. The residue was treated with toluene (3 × 20 mL), washed with water (100 mL) and recrystallized from ethanol. A white powder was obtained; mp: 100–102 °C. Yield: 41%. IR (KBr) cm^{-1}: 3426 (N–H), 1756 (C=O), 1663 (C=N). ^1H NMR (400 MHz, $CDCl_3$) δ: 2.34 (s, 3H, $SeCH_3$); 3.83 (s, 6H, OCH_3); 6.93 (d, 4H, $2H_2 + 2H_6$, $J_{2-3} = J_{6-5} = 8.7$ Hz); 7.11 (d, 4H, $H_3 + H_5$, $H_{3'} + H_{5'}$, $J_{2-3} = J_{6-5} = 8.7$ Hz); 12.18 (s, 1H, N–H). ^{13}C NMR (100 MHz, $CDCl_3$) δ: 8.8 (1C, $SeCH_3$); 56.3 (2C, $2OCH_3$); 115.1 (4C, $2C_2 + 2C_6$); 123.3 (6C, $2C_1 + 2C_3 + 2C_5$); 151.9 (1C, CONH); 153.3 (2C, $2C_1$); 157.8 (1C, CON); 162.9 (1C, CSe). MS (*m/z* % abundance): 219 (21), 191 (64), 165 (71), 124 (100), 109 (62), 81 (31). Elemental Analysis for $C_{18}H_{18}N_2O_6Se$, Calcd/Found (%): C: 49.55/49.43; H: 4.12/4.30; N: 6.41/6.04.

*4.1.11. Methyl N,N′-bis(4-methylphenoxycarbonyl) imidoselenocarbamate (**9**)*

From 4-methylphenyl chloroformate. The residue was purified by silica gel column chromatography (toluene/dioxane 90/10) to give **9** as white powder; mp: 100–102 °C. Yield: 30%. IR (KBr) cm^{-1}: 3426 (N–H), 1756 (C=O), 1637 (C=N). ^1H NMR (400 MHz, $CDCl_3$) δ: 2.22 (s, 3H, $SeCH_3$); 2.31 (s, 6H, $2CH_3$); 7.13 (d, 4H, $2H_2 + 2H_6$, $J_{2-3} = J_{6-5} = 8.0$ Hz); 7.23 (d, 4H, $2H_3 + 2H_5$, $J_{2-3} = J_{6-5} = 8.0$ Hz). ^{13}C NMR (100 MHz, $CDCl_3$) δ: 6.9 (1C, $SeCH_3$); 21.2 (2C, $2CH_3$); 122.3 (2C, $C_2 + C_6$); 130.5 (2C, $C_3 + C_5$); 134.7 (1C, C_4) 150.2 (1C, C_1); 153.0 (1C, CONH); 159.6 (1C, CON); 161.5 (1C, CSe). MS (*m/z* % abundance): 299 (9), 203 (44), 191 (100), 123 (15), 107 (75), 91 (22), 77 (27). Elemental Analysis for $C_{18}H_{18}N_2O_4Se \cdot 1/2HCl$, Calcd/Found (%): C: 51.03/51.58; H: 4.37/4.52; N: 6.61/7.02.

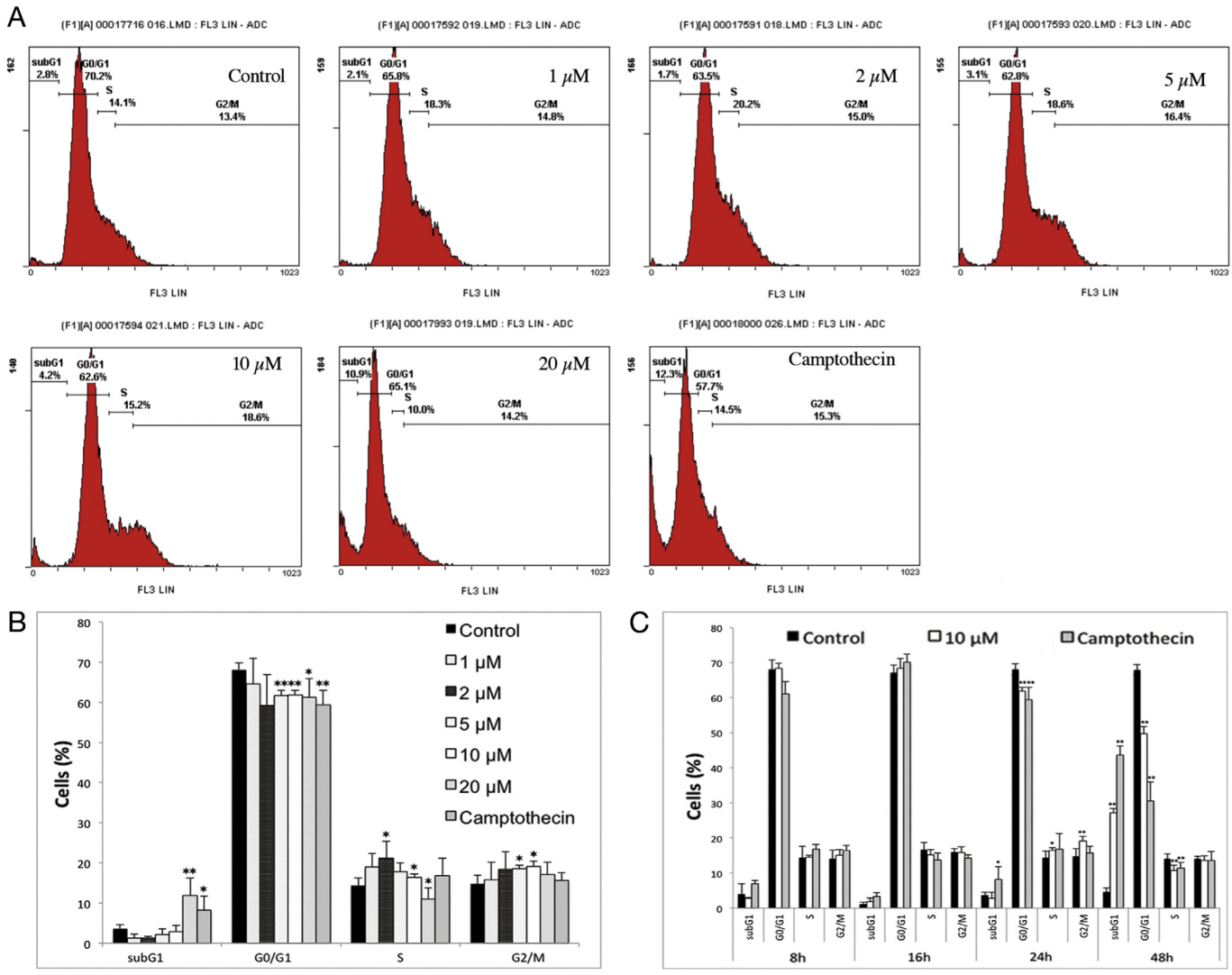

Fig. 7. Effect of compound **2** on cycle phase distribution in HTB-54 cells. Cell cycle analysis of the cells was performed by TUNEL as described in Experimental protocols. (**A**) Flow cytometry analysis of a representative experiment performed with cells treated with 1–20 μM **2** or vehicle (control) for 24 h. (**B**) Percentage of cells in each phase of the cell cycle after incubation of the cells in the presence or absence (control) of **2** (1–20 μM) for 24 h. (**C**) Time course analysis of cell cycle phase distribution of HTB-54 cell cultures treated with 10 μM of **2**. Camptothecin was used as a positive control. Results are presented as the mean ± SEM of three independent experiments performed in duplicate. $^{*}p < 0.05$ and $^{**}p < 0.01$ respect to control cells.

*4.1.12. Methyl N,N′-bis(4-chlorophenoxycarbonyl) imidoselenocarbamate (**10**)*

From 4-chlorophenyl chloroformate. The residue was treated with toluene (3 × 20 mL), washed with water (100 mL) and recrystallized from ethanol. A white powder was obtained; mp: 120–122 °C. Yield: 5%. IR (KBr) cm^{-1}: 3430 (N–H), 1761 (C=O), 1664 (C=N). ^{1}H NMR (400 MHz, $CDCl_3$) δ: 2.34 (s, 3H, $SeCH_3$); 7.15 (d, 4H, $2H_2 + 2H_6$, $J_{2-3} = J_{6-5} = 8.8$ Hz); 7.39 (d, 4H, $2H_3 + 2H_5$, $J_{2-3} = J_{6-5} = 8.8$ Hz); 12.16 (s, 1H, N–H). ^{13}C NMR (100 MHz, $CDCl_3$) δ: 8.9 (1C, $SeCH_3$); 117.8 (4C, $2C_2 + 2C_6$); 124.6 (6C, $2C_3 + 2C_4 + 2C_5$); 130.3 (2C, $2C_1$); 153.1 (1C, CONH); 160.1 (1C, CON); 162.8 (1C, CSe). MS (*m/z* % abundance): 319 (9), 191 (100), 128 (81). Elemental Analysis for $C_{16}H_{12}Cl_2N_2O_4Se$, Calcd/Found (%): C: 43.05/42.80; 2.69/2.83; N: 6.28/6.32.

*4.1.13. Methyl N,N′-bis(4-fluorophenoxycarbonyl) imidoselenocarbamate (**11**)*

From 4-fluorophenyl chloroformate. The residue was treated with toluene (3 × 20 mL), washed with water (100 mL) and recrystallized from ethanol. A white powder was obtained; mp: 132–134 °C. Yield: 14%. IR (KBr) cm^{-1}: 3430 (N–H), 1761 (C=O), 1664 (C=N). ^{1}H NMR (400 MHz, $CDCl_3$) δ: 2.34 (s, 3H, $SeCH_3$); 7.15 (m, 8H, H_{arom}); 12.17 (s, 1H, N–H). ^{13}C NMR (100 MHz, $CDCl_3$) δ: 8.9 (1C, $SeCH_3$); 117.0 (d, 4C, $2C_3 + 2C_5$, $J^{2}_{C-F} = 24$ Hz); 124.4 (d, 4C, $2C_2 + 2C_6$, $J^{3}_{C-F} = 24$ Hz); 130.9 (d, 2C, $2C_4$, $J^{1}_{C-F} = 286$ Hz); 147.2 (2C, $2C_1$); 154.1 (1C, CONH); 161.8 (1C, CON); 162.9 (1C, CSe). MS (*m/z* % abundance): 303 (49), 191 (100), 112 (72), 95 (61), 57 (24). Elemental Analysis for $C_{16}H_{12}F_2N_2O_4Se$, Calcd/Found (%): C: 46.49/46.10; H: 2.91/2.92; N: 6.78/7.08.

*4.1.14. Methyl N,N′-bis(benzyloxycarbonyl)imidoselenocarbamate (**12**)*

From benzyl chloroformate. The residue was purified by silica gel column chromatography (toluene/dioxane 90/10) to give **12** as white powder; mp: 68–70 °C. Yield: 13%. IR (KBr) cm^{-1}: 3430 (N–H), 1742 (C=O), 1654 (C=N). ^{1}H NMR (400 MHz, $CDCl_3$) δ: 2.30 (s, 3H, $SeCH_3$); 5.22 (s, 4H, $2CH_2$); 7.40 (m, 10H, H_{arom}); 11.98 (s, 1H, NH). ^{13}C NMR (100 MHz, $CDCl_3$) δ: 8.5 (1C, $SeCH_3$); 68.4 (2C, $2CH_2$); 129.1 (10C, $2C_2 + 2C_6 + 2C_3 + 2C_4 + 2C_5$); 136.4 (2C, $2C_1$); 153.0 (1C, CONH); 159.6 (1C, CON); 161.5 (1C, CSe). MS (*m/z* % abundance):

406 ($M^{+\bullet}$), 203 (6), 107 (6), 91 (100), 77 (6), 65 (8). Elemental Analysis for $C_{18}H_{18}N_2O_4Se$, Calcd/Found (%): C: 53.33/53.07; H: 4.44/4.48; N: 6.91/6.78.

4.1.15. Methyl N,N′-bis(4-nitrobenzyloxycarbonyl) imidoselenocarbamate (**13**)

From 4-nitrobenzyl chloroformate. The residue was treated with toluene (3 × 20 mL), washed with water (100 mL) and recrystallized from ethanol. A white powder was obtained; mp: 158–159 °C. Yield: 6%. IR (KBr) cm^{-1}: 3404 (N–H), 1751 (C=O), 1647 (C=N). ^1H NMR (400 MHz, DMSO) δ: 2.15 (s, 3H, $SeCH_3$); 5.29 (s, 4H, $2CH_2$); 7.68 (d, 4H, $2H_2 + 2H_6$, $J_{2-3} = J_{6-5} = 8.0$ Hz); 8.25 (d, 4H, $2H_3 + 2H_5$, $J_{2-3} = J_{6-5} = 8.0$ Hz); 11.44 (s, 1H, NH). ^{13}C NMR (100 MHz, $CDCl_3$) δ: 8.6 (1C, $SeCH_3$); 67.0 (2C, $2CH_2$); 124.4 (4C, $2C_3 + 2C_5$); 129.6 (4C, $2C_2 + 2C_6$); 144.2 (2C, $2C_1$); 148.0 (2C, $2C_4$); 153.0 (1C, CONH); 159.6 (1C, CON); 161.7 (1C, CSe). MS (*m/z* % abundance): 136 (100), 106 (27), 89 (37), 31 (31). Elemental Analysis for $C_{18}H_{16}N_4O_8Se$, Calcd/Found (%): C: 43.65/43.89; H: 3.16/2.99; N: 11.31/11.25.

4.1.16. Methyl N,N′-bis(9H-fluoren-9-ylmethoxycarbonyl) imidoselenocarbamate (**14**)

From fluorenylmethyloxycarbonyl chloride. The residue was treated with toluene (3 × 20 mL), washed with water (100 mL) and recrystallized from ethanol. A white powder was obtained; mp: 146–147 °C. Yield: 24%. IR (KBr) cm^{-1}: 3431 (N–H), 3066 (C–H_{arom}), 2931 (C–H_{ali}), 1751 (C=O), 1643 (C=N). ^1H NMR (400 MHz, $CDCl_3$) δ: 1.28 (m, 2H, $2H_9$); 2.41 (s, 3H, $SeCH_3$); 4.49 (d, 4H, 2 CH_2, $J_{CH_{2-9}} = 7.0$ Hz); 7.36 (t, 4H, $2H_2 + 2H_7$, $J_{1-2} = J_{2-3} = J_{6-7} = J_{7-8} = 7.0$ Hz); 7.44 (t, 4H, $2H_3 + 2H_6$, $J_{2-3} = J_{3-4} = J_{5-6} = J_{6-7} = 7.0$ Hz); 7.65 (d, 4H, $2H_1 + 2H_8$, $J_{1-2} = J_{7-8} = 7.0$ Hz); 7.65 (d, 4H, $2H_4 + 2H_5$, $J_{3-4} = J_{5-6} = 7.0$ Hz); 12.08 (s, 1H, N–H). ^{13}C NMR (100 MHz, $CDCl_3$) δ: 8.6 (1C, $SeCH_3$); 47.1 (2C, $2C_9$); 68.2 (2C, $2CH_2$); 121.1 (4C, $2C_1 + 2C_8$); 26.0 (4C, $2C_2 + 2C_7$); 128.5 (8C, $2C_3 + 2C_4 + 2C_5 + 2C_6$); 153.1 (1C, CONH); 159.5 (1C, CON); 161.7 (1C, CSe). MS (*m/z* % abundance): 368 (45), 191 (100), 163 (48), 135 (24), 97 (22), 57 (56). Elemental Analysis for $C_{32}H_{26}N_4O_4Se$, Calcd/Found (%): C: 66.09/66.42; H: 4.48/4.54; N: 4.82/4.85.

4.1.17. Methyl N-(1,1-dioxidebenzo[b]thiophen-2-yloxycarbonyl) imidoselenocarbamate (**15**)

From 1,1-dioxidebenzo[b]thiophen-2-chloroformate. White powder; mp: 177–178 °C. Yield: 78%. IR (KBr) cm^{-1}: 3419 (N–H), 2932 (C–H_{ali}), 1676 (C=O), 1638 (C=N). ^1H NMR (400 MHz, DMSO-d_6) δ: 2.21 (s, 3H, $SeCH_3$); 5.01 (s, 2H, CH_2); 7.52 (s, 1H, H_3); 7.62 (m, 2H, $H_4 + H_5$); 7.70 (t, 1H, H_6, $J_{6-7} = 7.4$ Hz, $J_{6-5} = 7.4$ Hz); 7.87 (d, 1H, H_7, $J_{7-6} = 7.4$ Hz); 8.95 (s, 2H, NH_2) ^{13}C NMR (100 MHz, DMSO-d_6) δ: 6.8 (1C, $SeCH_3$); 57.2 (1C, CH_2); 122.1 (1C, C_7); 126.9 (1C, C_4); 130.7 (1C, C_6); 130.9 (1C, C_a); 131.6 (1C, C_3); 135.1 (1C, C_5); 137.4 (1C, C_2); 140.1 (1C, C_b); 161.8 (1C, CO); 172.6 (1C, CSe). MS (*m/z* % abundance): 274 (17), 196 (18), 179 (87), 131 (100), 115 (64), 103 (28), 77 (26), 69 (21). Elemental Analysis for $C_{12}H_{12}N_2O_4SSe$, Calcd/Found (%): C: 40.11/39.67; H: 3.34/3.51; N: 7.80/7.71.

4.1.18. Methyl N-(4-methylphenoxycarbonyl) imidoselenocarbamate (**16**)

Yellow powder; mp: 100–102 °C. Yield: 47%. IR (KBr) cm^{-1}: 3444 (N–H), 1749 (C=O), 1637 (C=N). ^1H NMR (400 MHz, $CDCl_3$) δ: 2.37 (s, 6H, $SeCH_3 + CH_3$); 7.08 (d, 2H, $H_2 + H_6$, $J_{2-3} = J_{6-5} = 8.0$ Hz); 7.22 (d, 2H, $H_3 + H_5$, $J_{2-3} = J_{6-5} = 8.0$ Hz). ^{13}C NMR (100 MHz, $CDCl_3$) δ: 6.9 (1C, $SeCH_3$); 21.2 (1C, CH_3); 122.3 (2C, $C_2 + C_6$); 130.5 (2C, $C_3 + C_5$); 134.7 (1C, C_4) 150.2 (1C, C_1); 161.2 (1C, CO); 173.0 (1C, CSe); MS (*m/z* % abundance): 272 ($M^{+\bullet}$, 2), 203 (33), 191 (88), 165 (26), 123 (16), 107 (100), 91 (27), 77 (40), 69 (17). Elemental Analysis for $C_{10}H_{12}N_2O_2Se$, Calcd/Found (%): C: 44.28/44.22; H: 4.43/3.97; N: 10.33/10.41.

4.2. Biological evaluation

4.2.1. Cytotoxic and antiproliferative activities

The cytotoxic effect of each substance was tested at five different concentrations ranging between 0.01 and 100 μM. Each substance was initially dissolved in DMSO at a concentration of 0.01 M and serial dilutions were prepared using culture medium. The plates with cells from the different lines, to which medium containing the substance under test was added, were incubated for 72 h at 37 °C in a humidified atmosphere containing 5% CO_2.

Human cell lines were provided by the European Collection of Cell Cultures (ECACC) or the American Type Culture Collection (ATCC). Eight cell lines were used: CCRF-CEM (lymphoblastic leukaemia), K-562 (lymphocytic leukaemia), HT-29 (colon carcinoma), HTB-54 (lung carcinoma), PC-3 (prostate carcinoma), MCF-7 (breast adenocarcinoma), 184B5 (non-malignant, mammary gland derived) and BEAS-2B (non-malignant, derived from bronchial epithelium). CCRF-CEM, HT-29, PC-3, K-562 and HTB-54 cells were grown in RPMI 1640 medium (Invitrogen) supplemented with 10% foetal calf serum, 2 mM L-glutamine, 100 units/mL penicillin, 100 μg/mL streptomycin and 10 mM HEPES buffer (pH = 7.4). MCF-7 cells were grown in EMEM medium (Clonetics) supplemented with 10% foetal calf serum, 2 mM L-glutamine, 100 units/mL penicillin and 100 μg/mL streptomycin. 184B5 cells were grown in Hams F-12/DMEM (50:50) supplemented is described by Li et al. [44]. BEAS-2B were grown in 25 mL foetal bovine serum (FBS), 5 mL insulin–transferrin–sodium selenite (ITS), 1 mL hydrocortisone, 10 mL sodium pyruvate, 5 mL glutamine, 5 mL penicillin/gentamicin, 10 μL epidermal growth factor (EGF), and 150 μL retinoic acid (1 μM). Cytotoxicity was then determined by the MTT method [38]. Results were obtained from at least 3 independent experiments performed in quadruplicate and are expressed as GI_{50}, the concentration that reduces by 50% the growth of treated cells with respect to untreated controls, TGI, the concentration that completely inhibits cell growth, and LC_{50}, the concentration that kills 50% of the cells.

4.2.2. Evaluation of cell cycle progression and cell death

For lung carcinoma HTB-54 cells, both the apoptotic status and cell cycle analysis of the cells were determined using the *Apo-Direct* kit (BD Pharmingen) based on the TUNEL technique, under the conditions described by the manufacturer. Briefly, for fixation step cells were suspended in 1% paraformaldehyde in PBS (pH 7.4) at a concentration of 1×10^6 cells/mL, incubated on ice for 1 h, collected by centrifugation, washed, adjusted to 1×10^6 cells/mL in 70% ice-cold ethanol and incubated at −20 °C for 30 min. After fixation, cells were recovered by centrifugation, washed, solved in FITC dUTP-DNA labelling solution and incubated for 1 h at 37 °C. Cells were then rinsed, solved in PI/RNase staining buffer, incubated in the dark for 30 min at RT and analysed using a Coulter Epics XL flow cytometer.

The apoptotic status of leukaemia CCRF-CEM cells was evaluated by measuring the exposure of phosphatidylserine on the cell membranes using the *Annexin V-FITC Kit* (BD Pharmingen). Briefly, 5×10^5 cells were pelleted and washed in PBS. Cells were then stained with Annexin V-FITC and propidium iodide for 15 min at 4 °C in the dark and analysed using a Coulter Epics XL flow cytometer. For cell cycle analysis in CCRF-CEM cells, cells were fixed in 70% ethanol at 4 °C for 20 min and DNA content was measured by staining with propidium iodide (50 μM).

The statistical analysis was carried out using the two-tailed Student's paired *t*-test.

Acknowledgements

The authors wish to express their gratitude to the Ministerio de Educación y Ciencia, Spain (SAF 2009-07744) and to CAN Foundation (12,566) for financial support for the project. We thank Nathaniel Edward Bennet Saidu for carefully reading the manuscript.

Appendix A. Supplementary data

Supplementary data related to this article can be found at http://dx.doi.org/10.1016/j.ejmech.2014.06.076.

References

[1] R. Siegel, D. Naishadham, A. Jemal, Cancer statistics 2013, CA Cancer J. Clin. 63 (2013) 11–30.
[2] G.L. Kelly, A. Strasser, The essential role of evasion from cell death in cancer, Adv. Cancer Res. 111 (2011) 39–96.
[3] A. Nishina, H. Kimura, K. Kozawa, G. Sommen, F. Favero, H. Heimgartner, M. Koketsu, S. Furukawa, 3-(2,6-Dimethylphenyl)-2-selenoxo-1,3-thiazolidin-4-one suppresses hydrogen peroxide induced cytotoxicity on PC12 cells via activation of MAPK, Int. J. Toxicol. 30 (2011) 690–699.
[4] P. Arsenyan, E. Paegle, S. Belyakov, I. Shestakova, E. Jaschenko, I. Domracheva, J. Popelis, Synthesis, structure and cytotoxicity of 3-C, N, S, Se substituted benzo[*b*]selenophene derivatives, Eur. J. Med. Chem. 46 (2011) 3434–3443.
[5] M.A. Crampsie, M.K. Pandev, D. Desai, J. Spallholz, S. Amin, A.K. Sharma, Phenylalkyl isoselenocyanates vs phenyllalkyl isothiocyanates: thiol reactivity and its implications, Chem. Biol. Interact. 200 (2012) 28–37.
[6] F. Nedel, V.F. Campos, D. Alves, A.J. McBride, O.A. Dellagostin, T. Collares, L. Savegnago, F.K. Seixas, Substituted diaryl diselenides: cytotoxic and apoptotic effect in human colon adenocarcinoma cells, Life Sci. 91 (2012) 345–352.
[7] R. Gowda, S.V. Madhunapantula, D. Desai, S. Amin, G.P. Robertson, Selenium-containing histone deacetylase inhibitors for melanoma management, Cancer Biol. Ther. 13 (2012) 756–765.
[8] R. Gowda, S.V. Madhunapantula, D. Desai, S. Amin, G.P. Robertson, Simultaneous targeting of COX-2 and AKT using selenocoxib-1-GSH to inhibit melanoma, Mol. Cancer Ther. 12 (2013) 3–15.
[9] A. dos Santos Edos, E. Hamel, R. Bai, J.C. Burnett, C.S. Tozatti, D. Bogo, R.T. Perdomo, A.M. Antunes, M.M. Marques, M.F. Matos, D.P. de Lima, Synthesis and evaluation of diaryl sulfides and diaryl selenide compounds for antitubulin and cytotoxic activity, Bioorg. Med. Chem. Lett. 23 (2013) 4669–4673.
[10] M. Font, A. Zuazo, E. Ansó, D. Plano, C. Sanmartín, J.A. Palop, J.J. Martínez-Irujo, Novel structural insights for imidoselenocarbamates with antitumoral activity related to their ability to generate methylselenol, Bioorg. Med. Chem. 20 (2012) 5110–5116.
[11] H. Zeng, W.H. Cheng, L.K. Johnson, Methylselenol, a selenium metabolite, modulates p53 pathway and inhibits the growth of colon cancer xenografts in Balb/c mice, J. Nutr. Biochem. 24 (2013) 776–780.
[12] B.D. Van Rite, J.J. Krais, M. Cherry, V.I. Sikavitsas, C. Kurkjian, R.G. Harrison, Antitumor activity of an enzyme prodrug therapy targeted to the breast tumor vasculature, Cancer Investig. 31 (2013) 505–510.
[13] Y. Zhan, B. Cao, Y. Qi, S. Liu, Q. Zhang, W. Zhou, D. Xu, H. Lu, O. Sartor, W. Kong, H. Zhang, Y. Dong, Methylselenol prodrug enhances MDV3100 efficacy for treatment of castration-resistant prostate cancer, Int. J. Cancer 133 (2013) 2225–2233.
[14] D. Plano, C. Sanmartín, E. Moreno, C. Prior, A. Calvo, J.A. Palop, Novel potent organoselenium compounds as cytotoxic agents in prostate cancer cells, Bioorg. Med. Chem. Lett. 17 (2007) 6853–6859.
[15] C. Sanmartín, D. Plano, E. Domínguez, M. Font, A. Calvo, C. Prior, I. Encío, J.A. Palop, Synthesis and pharmacological screening of several aroyl and heteroaroyl selenylacetic acid derivatives as cytotoxic and antiproliferative agents, Molecules 14 (2009) 3313–3338.
[16] D. Plano, Y. Baquedano, E. Ibáñez, I. Jiménez, J.A. Palop, J.E. Spallholz, C. Sanmartín, Antioxidant-prooxidant properties of a new organoselenium compound library, Molecules 15 (2010) 7292–7312.
[17] D. Plano, E. Moreno, M. Font, I. Encío, J.A. Palop, C. Sanmartín, Synthesis and in vitro anticancer activities of some selenadiazole derivatives, Arch. Pharm. 343 (2010) 680–691.
[18] E. Ibáñez, D. Plano, M. Font, A. Calvo, C. Prior, J.A. Palop, C. Sanmartín, Synthesis and antiproliferative activity of novel symmetrical alkylthio- and alkylseleno-imidocarbamates, Eur. J. Med. Chem. 46 (2011) 265–274.
[19] D. Plano, E. Ibáñez, A. Calvo, J.A. Palop, C. Sanmartín, Novel library of selenocompounds as kinase modulators, Molecules 16 (2011) 6349–6364.
[20] E. Moreno, D. Plano, I. Lamberto, M. Font, I. Encío, J.A. Palop, C. Sanmartín, Sulfur and selenium derivatives of quinazoline and pyrido[2,3-*d*]pyrimidine: synthesis and study of their potential cytotoxic activity in vitro, Eur. J. Med. Chem. 47 (2012) 283–298.
[21] E. Ibáñez, M. Stoedter, P.J. Hofmann, D. Plano, A. Calvo, P.A. Nguewa, J.A. Palop, C. Sanmartín, L. Schomburg, Structure- and cell-specific effects of imidoselenocarbamates on selenoprotein expression and activity in liver cells in culture, Metallomics 4 (2012) 1297–1307.
[22] E. Domínguez-Álvarez, D. Plano, M. Font, A. Calvo, C. Prior, C. Jacob, J.A. Palop, C. Sanmartín, Synthesis and antiproliferative activity of novel selenoester derivatives, Eur. J. Med. Chem. 73 (2014) 153–166.
[23] I. Lamberto, D. Plano, E. Moreno, M. Font, J.A. Palop, C. Sanmartín, I. Encío, Bisacylimidoselenocarbamates cause G2/M arrest associated with the modulation of CDK1 and Chk2 in human breast cancer MCF-7 cells, Curr. Med. Chem. 20 (2013) 1609–1619.
[24] M. Font, E. Lizarraga, E. Ibáñez, D. Plano, C. Sanmartín, J.A. Palop, Structural variations on antitumour agents derived from bisacylimidoselenocarbamate. A proposal for structure-activity relationships based on the analysis of conformational behavior, Eur. J. Med. Chem. 66 (2013) 489–498.
[25] H.S. Byun, R. Bittman, P. Samadder, G. Arthur, Synthesis and antitumor activity of ether glycerophospholipids bearing a carbamate moiety at the sn-2 position: selective sensitivity against prostate cancer cell lines, ChemMedChem 5 (2010) 1045–1052.
[26] J.J. Wilson, S.J. Lippard, Synthesis, characterization, and cytotoxicity of platinum(IV) carbamate complexes, Inorg. Chem. 50 (2011) 3103–3115.
[27] J.F. Liu, C.Y. Sang, X.H. Xu, L.L. Zhang, X. Yang, L.L. Hui, J.:B. Zhang, S.W. Chen, Synthesis and cytotoxic activity on human cancer cells of carbamate derivatives of 4β-(1,2,3-triazol-1-yl)podophyllotoxin, Eur. J. Med. Chem. 64 (2013) 621–628.
[28] C.Y. Sang, J.F. Liu, W.W. Qin, J. Zhao, L. Hui, Y.X. Jin, S.W. Chen, Synthesis and evaluation of the apoptosis inducing and CT DNA interaction properties of a series of 4β-carbamoyl-4′-O-demethylepipodophyllotoxins, Eur. J. Med. Chem. 70 (2013) 59–67.
[29] J.K. Fauser, L.D. Prisciandaro, A.G. Cummins, G.S. Howarth, Fatty acids as potential adjunctive colorectal chemotherapeutic agents, Cancer Biol. Ther. 11 (2011) 724–731.
[30] B.S. Chhikara, N. St Jean, D. Mandal, A. Kumar, K. Parang, Fatty acyl amide derivatives of doxorubicin: synthesis and in vitro anticancer activities, Eur. J. Med. Chem. 46 (2011) 2037–2042.
[31] A. Tesei, G. Brigliadori, S. Carloni, F. Fabbri, P. Ulivi, C. Arienti, A. Sparatore, P. Del Soldato, A. Pasini, D. Amadori, R. Silvestrini, W. Zoli, Organosulfur derivatives of the HDAC inhibitor valproic acid sensitize human lung cancer cell lines to apoptosis and to cisplatin cytotoxicity, J. Cell. Physiol. 227 (2012) 3389–3396.
[32] R. Hegedüs, M. Manea, E. Orbán, I. Szabó, E. Kiss, E. Sipos, G. Halmos, G. Mezo, Enhanced cellular uptake and in vitro antitumor activity of short-chain fatty acid acylated daunorubicin-GnRH-III bioconjugates, Eur. J. Med. Chem. 56 (2012) 155–165.
[33] J.K. Fauser, G.M. Matthews, A.G. Cummins, G.S. Howarth, Induction of apoptosis by the medium-chain length fatty acid lauric acid in colon cancer cells due to induction of oxidative stress, Chemotherapy 59 (2013) 214–224.
[34] C.T. Yen, C.C. Wu, J.C. Lee, S.L. Chen, S.L. Morris-Natschke, P.W. Hsieh, Y.C. Wu, Cytotoxic N-(fluorenyl-9-methoxycarbonyl) (Fmoc)-dipeptides: structure-activity relationships and synergistic studies, Eur. J. Med. Chem. 45 (2010) 2494–2502.
[35] A.A. Sagardoy, M.J. Gil, R. Villar, M.J. Viñas, A. Arrazola, I. Encío, V. Martínez-Merino, Benzo[*b*]thiophene-6-carboxamide 1,1,-dioxides: inhibitors of human cancer cell growth at nanomolar concentrations, Bioorg. Med. Chem. 18 (2010) 5701–5707.
[36] I. Iriepa, F.J. Villasante, E. Gálvez, J. Bellanato, A. Martín, P. Gómez-Sal, Synthesis, spectroscopic and crystallographic study of some carbamates from an azabicyclic chloroformate and primary heterocyclic amines, New J. Chem. 28 (2004) 618–624.
[37] C.A. Terraza, L.H. Tagle, A. Leiva, J.C. Vega, Synthesis and characterization of 4,4′-(dimethylsilylene) bis(phenyl chloroformate) and 4,4′-(dimethylgermylene)bis(phenyl chloroformate) and their use in the synthesis of poly(-urethanes), Polym. Bull. 52 (2004) 101–107.
[38] I. Encío, D.J. Morré, R. Villar, M.J. Gil, V. Martínez-Merino, Benzo[*b*]thiophenesulphonamide 1,1-dioxide derivatives inhibit tNOX activity in a redox state-dependent manner, Br. J. Cancer 92 (2005) 690–695.
[39] E.M. Acton, V.L. Narayanan, P.A. Risbood, R.H. Shoemaker, D.T. Vistica, M.R. Boyd, J. Med. Chem. 37 (1994) 2185–2189.
[40] http://www.molinspiration.com/services/properties.html, 2012.
[41] P. Chen, L. Wang, N. Li, Q. Liu, J. Ni, Comparative proteomics analysis of sodium selenite-induced apoptosis in human prostate cancer cell, Metallomics 5 (2013) 541–550.
[42] M.A. Fernández-Herrera, J. Sandoval-Ramírez, L. Sánchez-Sánchez, H. López-Muñoz, M.L. Escobar-Sánchez, Probing the selective antitumor activity of 22-oxo-26-selenocyanocholestane derivatives, Eur. J. Med. Chem. 74 (2014) 451–460.
[43] E. Freilich, J. Rudno-Rudznska, K. Janiszewski, L. Salomon, K. Kotulski, O. Pelzer, Z. Grzebieniak, R. Tarnagua, W. Kielang, Caspases and their role in gastric cancer, Adv. Clin. Exp. Med. 22 (2013) 593–602.
[44] Y. Li, J. Pan, J.L. Li, J.H. Lee, C. Tunkey, K. Saraf, J.C. Garbe, M.Z. Whitley, S.A. Jelinsky, M.R. Stampfer, S.A. Haney, Transcriptional changes associated with breast cancer occur as normal human mammary epithelial cells overcome senescence barriers and become immortalized, Mol. Cancer 18 (2007) 6–7.